

The Second-Parameter Effect in Metal-Rich Globular Clusters

A. V. Sweigart and M. Catelan

NASA/Goddard Space Flight Center

Laboratory for Astronomy and Solar Physics, Code 681

Greenbelt, MD 20771

e-mail: sweigart@bach.gsfc.nasa.gov, catelan@stars.gsfc.nasa.gov

ABSTRACT

Recent *Hubble Space Telescope* observations have found that the horizontal branches (HB's) in the metal-rich globular clusters NGC 6388 and NGC 6441 slope upward with decreasing $B-V$. Such a slope is not predicted by canonical HB models and cannot be produced by either a greater cluster age or enhanced mass loss along the red-giant branch (RGB). The peculiar HB morphology in these clusters may provide an important clue for understanding the second-parameter effect.

We have carried out extensive evolutionary calculations and numerical simulations in order to explore three non-canonical scenarios for explaining the sloped HB's in NGC 6388 and NGC 6441: i) A high cluster helium abundance scenario, where the HB evolution is characterized by long blue loops; ii) A rotation scenario, where internal rotation during the RGB phase increases the HB core mass; iii) A helium-mixing scenario, where deep mixing on the RGB enhances the envelope helium abundance. All three of these scenarios predict sloped HB's with anomalously bright RR Lyrae variables. We compare this prediction with the properties of the two known RR Lyrae variables in NGC 6388. Additional observational tests of these scenarios are suggested.

Subject headings: Stars: evolution — stars: horizontal-branch — stars: variables: other — Galaxy: globular clusters: individual (NGC 6388, NGC 6441)

1. Introduction

Many years ago Sandage & Wildey (1967) and van den Bergh (1967) discovered that the horizontal-branch (HB) morphology in the Galactic globular clusters (GC's) does not correlate tightly with the cluster metallicity. While theory and observation agree that the HB morphology on average becomes redder with increasing metallicity, there are many examples of GC's having very similar metallicities but markedly different HB morphologies, e.g., M3 versus M13, NGC 362 versus NGC 288. Thus some parameter besides metallicity must be affecting the evolution of the

HB stars in these clusters. Indeed, theoretical HB models show that there are many possible “second parameter” candidates, e.g., the GC age, mass loss along the red-giant branch (RGB), helium abundance Y , alpha-element enhancement $[\alpha/\text{Fe}]$, and rotation (Fusi Pecci & Bellazzini 1998).

Recent *Hubble Space Telescope* (HST) observations have revealed that the metal-rich GC’s NGC 6388 and NGC 6441 contain a significant population of blue HB (BHB) stars and therefore exhibit a pronounced second-parameter effect (Piotto et al. 1997; Rich et al. 1997). From their analysis, Rich et al. concluded that neither a greater age nor enhanced RGB mass loss due to dynamical effects could satisfactorily account for the BHB populations in these GC’s. Understanding the origin of these BHB stars has important implications for determining the formation history of the Galaxy and for interpreting the integrated spectra of the old metal-rich stellar populations in elliptical galaxies. If, for example, age were the second parameter in these GC’s, then NGC 6388 and NGC 6441 would be among the oldest, if not the oldest, GC’s in the Galaxy.

Sweigart & Catelan (1998) pointed out that the HB’s of NGC 6388 and NGC 6441 have a pronounced upward slope with decreasing $B - V$, with the mean luminosity at the top of the blue tail being nearly 0.5 mag brighter in V than the well-populated red HB (RHB) clump. A similar upward slope is also present in the RHB itself (Piotto et al. 1997). As we shall see, such upward sloping HB’s cannot be explained within the framework of canonical theory. More specifically, they cannot be attributed to differences in age or RGB mass loss—the two most prominent second-parameter candidates. We emphasize therefore that these GC’s may provide a crucial clue for understanding the second-parameter effect.

In this *Letter* we will investigate the following non-canonical scenarios for explaining the BHB populations and, in particular, the sloped HB’s in NGC 6388 and NGC 6441:

1. *High Y scenario*, where a high helium abundance at the time of GC formation leads to unusually long blue loops during the HB evolution;
2. *Rotation scenario*, where internal rotation increases the HB core mass, making the HB both bluer and brighter;
3. *Helium-mixing scenario*, where deep mixing along the RGB increases the HB envelope helium abundance, also leading to bluer and brighter HB stars.

We will explore each of these possibilities under the simplest possible assumptions and will show that each can produce sloped HB’s resembling those in NGC 6388 and NGC 6441.

We begin in Sec. 2 by discussing the failure of the canonical models to explain the observed HB’s in NGC 6388 and NGC 6441; in Sec. 3, we describe each of the above non-canonical scenarios in more detail; in Sec. 4, we show that the RR Lyraes in NGC 6388 are brighter than field

variables of similar $[\text{Fe}/\text{H}]$, in agreement with these scenarios. Finally, in Sec. 5 we suggest some observational tests to discriminate among these scenarios.

2. Canonical HB Morphology

In order to explore the HB morphology predicted by canonical models for NGC 6388 and NGC 6441, we have constructed a grid of HB sequences with a main-sequence helium abundance $Y_{\text{MS}} = 0.23$ and a scaled-solar heavy-element abundance $Z = 0.006$ (i.e., $[\text{Fe}/\text{H}] = -0.5$), using the stellar evolution code described by Sweigart (1997). Adopting the Kurucz (1992) color-temperature transformations and bolometric corrections, we first computed an HB simulation with the mean mass $\langle M_{\text{HB}} \rangle$ for the Gaussian mass distribution and the mass dispersion σ_M chosen to give a well-populated red and blue HB. This canonical simulation, shown in Fig. 1, predicts a completely flat HB morphology, unlike the observed HB’s in NGC 6388 and NGC 6441. In order to explore any dependence on metallicity, we also carried out extensive model computations for $Z = 0.002$ and $Z = 0.01716$ ($= Z_{\odot}$), again failing to find any evidence for sloped HB’s.

The HB simulation in Fig. 1 indicates that the BHB population in NGC 6388 and NGC 6441 does not arise from either an older cluster age or greater RGB mass loss. While increasing the assumed age or RGB mass loss would move an RHB star blueward, it would not increase its luminosity. We conclude therefore that canonical theory does not provide a straightforward explanation for the observed HB morphology in these GC’s.

We have also investigated whether the slope of the RHB in NGC 6388 and NGC 6441 could be due to differential reddening, as has been claimed for several metal-rich GC’s (e.g., NGC 6539: Armandroff 1988; Pal 10: Kaisler, Harris, & MacLaughlin 1997; NGC 6553: Guarneri et al. 1998). Extensive HB simulations show that the differential reddening $\Delta E(B-V)$ would have to considerably exceed the amounts estimated by Piotto et al. (1997) in order to transform, say, a 47 Tuc-like RHB into the sloped HB’s found in NGC 6388 and NGC 6441. Moreover, the HB’s in NGC 6388 and NGC 6441 are sloped in each of the four WFPC2 chips, which would not be expected if differential reddening were the cause of the sloped RHB’s in the color-magnitude diagrams (CMD’s) of these GC’s.

Finally, we point out that inaccuracies in the transformation from the WFPC2 filter system to the “standard” Johnson-Cousins system are also unlikely to cause the sloped HB’s in NGC 6388 and NGC 6441, since the instrumental CMD’s clearly show sloped HB’s (Dorman 1998, priv. comm.). If the filter transformation were responsible, one would expect sloped HB’s in the HST CMD’s for other GC’s (e.g., 47 Tuc and NGC 2808) from Piotto et al. (1997) and Sosin et al. (1997), which is not the case.

3. Non-Canonical HB Morphology

The failure of canonical models to explain the observed HB morphology in NGC 6388 and NGC 6441 suggests that some non-canonical process may be operating in these metal-rich GC's. In this section, we will therefore discuss three non-canonical scenarios for producing sloped HB's, beginning with the possibility of a high cluster helium abundance.

3.1. High Y Scenario

RHB stars evolve along blue loops during most of their HB lifetime. Normally these loops cover only a small range in $B-V$. For larger helium abundances, however, these blue loops can become considerably longer, reaching higher effective temperatures and deviating more in luminosity from the zero-age HB (ZAHB) (Sweigart & Gross 1976). Thus, at least qualitatively, one would expect the HB for a sufficiently high Y to slope upward with decreasing $B-V$ (Catelan & de Freitas Pacheco 1996).

To test this possibility, we have constructed a grid of ≈ 350 HB sequences for $Y_{\text{MS}} = 0.23, 0.28, 0.33, 0.38$ and 0.43 and $Z = 0.002, 0.006$ and 0.01716 . For each (Y_{MS}, Z) combination we first evolved a star up the RGB without mass loss and then through the helium flash to obtain a ZAHB model at the red end of the HB. Lower mass ZAHB models were then obtained by removing mass from the envelope of this high mass ZAHB model. Not surprisingly, the HB simulations for $Y_{\text{MS}} = 0.23, 0.28$ and 0.33 did not show a significant slope. However, when Y_{MS} was increased to 0.38 and 0.43 , a pronounced HB slope close to that in NGC 6388 and NGC 6441 was found, as illustrated in Figs. 2a,b, respectively. There is also a hint of bimodality, as seen in the observed CMD's (Rich et al. 1997). In these simulations we did not try to reproduce the ratio of blue to red HB stars. This ratio depends on the choice of $\langle M_{\text{HB}} \rangle$ and σ_M , assumed here to be $0.02 M_{\odot}$.

The HB's predicted by this high Y scenario are quite bright, implying a large pulsation period for the RR Lyrae variables and a large value for the number ratio R of HB stars to RGB stars brighter than the mean RR Lyrae luminosity (Iben 1968). In addition, this scenario would imply a peculiar chemical enrichment history for NGC 6388 and NGC 6441, characterized by a very large enrichment law $\Delta Y/\Delta Z$ (cf. Shi 1995; Schramm 1997).

3.2. Rotation Scenario

Since the work of Mengel & Gross (1976) it has been known that rotation during the RGB phase can delay the helium flash. As reviewed by Renzini (1977), this would have two consequences for the subsequent HB evolution. First, it would increase the helium-core mass M_c and hence the HB luminosity. Second, it would lead to enhanced mass loss near the tip of the RGB and thus to a smaller HB envelope mass. The net effect would be a shift in the HB location towards higher

effective temperatures and luminosities. Thus, at least qualitatively, one might also expect a range in rotation to produce an upward sloping HB. Could this be the explanation for the sloped HB’s in NGC 6388 and NGC 6441?

To answer this question, one needs to know how much extra mass is lost at the tip of the RGB when M_c exceeds its canonical value. We determined this by evolving a number of sequences up the RGB for various values of the Reimers mass loss parameter η_R (cf. Reimers 1975; Fusi Pecci & Renzini 1976). In these sequences we turned off all helium burning, thereby permitting M_c to exceed its canonical value without igniting the helium flash. Using these sequences, we were able to determine how the final mass M decreases with increasing M_c for each value of η_R . The $M - M_c$ relations defined in this manner were then used to compute grids of HB sequences for $\eta_R = 0.1, 0.2, 0.3$ and 0.4 .

Two simulations for this rotation scenario are shown in Fig. 2 for $\eta_R = 0.2$ (panel c) and 0.4 (panel d). The red end of the HB in these simulations is populated by canonical models without rotation. The masses of these canonical models were used as the mean mass $\langle M_{\text{HB}} \rangle$ for defining the mass range $M < \langle M_{\text{HB}} \rangle$ covered by these simulations. Thus the blueward extension of the HB in Figs. 2c,d is driven solely by the increase in M_c and corresponding decrease in M . In both Figs. 2c,d the HB slopes upward, especially in the $\eta_R = 0.2$ case. Note, however, that the increase in M_c for the bluer HB stars is very large ($\gtrsim 0.1 M_\odot$), which, in turn, would require a very high main-sequence rotation rate.

3.3. Helium-Mixing Scenario

The observed abundance variations in GC red-giant stars indicate that these stars are able to mix nuclearly processed material from the vicinity of the hydrogen shell out to the surface, presumably as a result of internal rotation (Kraft 1994). In particular, the observed variations in aluminum require the mixing to penetrate into the hydrogen shell (Langer & Hoffman 1995; Cavallo, Sweigart, & Bell 1998). Thus any mixing process which dredges up aluminum will also dredge up helium. Besides increasing the envelope helium abundance Y_{HB} such mixing would also increase the RGB tip luminosity and thus the amount of mass loss. Consequently a red-giant star which undergoes such helium mixing will arrive on the HB with both a higher Y_{HB} and a lower mass and hence will be both hotter and brighter than the corresponding canonical star (Sweigart 1997, 1998). This suggests, at least qualitatively, that helium mixing might also lead to a sloped HB morphology.

To investigate this possibility, we have evolved a set of ≈ 100 sequences up the RGB and through the helium flash and HB phases for various amounts of helium mixing. Two cases were considered, namely, $(M, Y_{\text{MS}}, Z) = (0.95, 0.23, 0.006)$ and $(0.87, 0.28, 0.006)$, where the mass in each case corresponds to an age of 13 Gyr at the tip of the RGB. The η_R values used in these sequences were $0.4, 0.5$ and 0.6 .

Two of the helium-mixing simulations for $Y_{\text{MS}} = 0.23$ are presented in Figs. 2e,f. Each of these simulations covers the mass range $M < \langle M_{\text{HB}} \rangle$, where $\langle M_{\text{HB}} \rangle$ was taken to be the mass of a canonical model without helium mixing. As the helium mixing increases, the HB tracks shift blueward, giving rise to the pronounced upward slope evident in Figs. 2e,f. In fact, the HB slope in Fig. 2e slightly exceeds the observed slope in NGC 6388 and NGC 6441. There is, moreover, a hint of bimodality in this simulation. The helium abundance Y_{HB} near the instability strip in Fig. 2e is ≈ 0.34 .

4. Constraints from RR Lyrae Variables

We have compared the predictions of the above simulations in the period-temperature diagram with the two known RRab Lyrae variables in NGC 6388 (Silbermann et al. 1994). Temperatures were determined as in Catelan, Sweigart, & Borissova (1998; see also Catelan 1998). The result of one such comparison is given in Fig. 3, where we also plot field variables of similar metallicity as well as V9 in 47 Tuc (Storm et al. 1994). The $[\text{Fe}/\text{H}]$ values for the field variables are from Layden (1994); amplitudes and periods are taken from Blanco (1992), but in some cases from Sandage (1990). Blazhko variables were avoided. As one can clearly see, the variables in NGC 6388 and 47 Tuc have considerably longer periods and thus substantially higher luminosities than field stars of comparable metallicity. Moreover, the cluster variables seem to agree well with the displayed simulation, which in this case was taken from Fig. 2e.

5. Discussion

The results in this *Letter* demonstrate that canonical models fail to explain the sloped HB's in NGC 6388 and NGC 6441. This has the important implication that, at least for these GC's, the two most prominent second-parameter candidates—age and RGB mass loss—cannot account for the observed HB morphology. Simulations employing non-canonical models show that an increased initial GC helium abundance or a dispersion in the stellar rotational velocity (leading to a range in M_c or Y_{HB}) may account for the observed HB morphology in these two GC's. Finally, we find that the RR Lyrae variables in NGC 6388 and 47 Tuc are substantially brighter than field variables of comparable $[\text{Fe}/\text{H}]$ —in agreement with the non-canonical scenarios.

We can suggest a variety of observational tests for discriminating among the different non-canonical scenarios, including:

1. *Analysis of R-ratios*: the R ratios differ widely from one non-canonical scenario to the next, being largest for the high- Y case (Figs. 2a,b). A low R ratio (implying $Y_{\text{MS}} \lesssim 0.35$) for NGC 6388 and NGC 6441 would argue against the high- Y scenario;
2. *Deep photometry of NGC 6388 and NGC 6441*: this would determine whether the magnitude

difference between the RR Lyraes and the turnoff, “ ΔV ,” is larger than expected for a “47 Tuc-like” age, as predicted by the non-canonical scenarios;

3. *RR Lyrae survey*: NGC 6388 and NGC 6441 should be surveyed for RR Lyraes, in order to discover new variables, especially closer to the cluster centers, and to define better the pulsation properties of the known RR Lyraes. In addition, we suggest a study of the RR Lyraes in the metal-rich GC’s NGC 6304 (Hartwick, Barlow, & Hesser 1981; Layden 1995) and NGC 6652 (Ortolani, Bica, & Barbuy 1994);
4. *Surface gravities of blue HB stars*: $\log g$ measurements could discriminate among the different origins of the BHB stars in NGC 6388 and NGC 6441 (Crocker, Rood, & O’Connell 1988) and provide a strong constraint on whether the HB’s are indeed brighter than predicted by the canonical models;
5. *High-resolution spectroscopy of red giants*: RGB stars in NGC 6388 and NGC 6441 should be searched for evidence of deep mixing (cf. Kraft 1994);
6. *Planetary Nebula (PN) in NGC 6441*: the PN recently discovered by Jacoby et al. (1997) in NGC 6441 may be an invaluable diagnostic tool for constraining the models. Helium is moderately enhanced over the solar value in this PN, while oxygen is more depleted than in the super-oxygen-poor stars which are found in some more metal-poor GC’s and which are indicative of deep mixing (e.g., Kraft 1994). We speculate that this PN may be the progeny of a star that experienced helium mixing.

M.C. would like to thank B. Dorman and S. Ortolani for useful discussions. This research was supported in part by NASA grant NAG5-3028. This work was performed while M.C. held a National Research Council–NASA/GSFC Research Associateship.

REFERENCES

- Armandroff, T. E. 1988, *AJ*, 96, 588
- Blanco, V. M. 1992, *AJ*, 104, 734
- Catelan, M. 1998, *ApJ*, 495, L81
- Catelan, M., & de Freitas Pacheco, J. A. 1996, *PASP*, 108, 166
- Catelan, M., Sweigart, A. V., & Borissova, J. 1998, in *ASP Conf. Ser. 135, A Half Century of Stellar Pulsation Interpretations: A Tribute to Arthur N. Cox*, ed. P. A. Bradley & J. A. Guzik (San Francisco: ASP), 41
- Cavallo, R. M., Sweigart, A. V., Bell, R. A. 1998, *ApJ*, 492, 575
- Crocker, D. A., Rood, R. T., & O’Connell, R. W. 1988, *ApJ*, 332, 236
- Fusi Pecci, F., & Bellazzini, M. 1998, in *The Third Conference on Faint Blue Stars*, ed. A. G. D. Philip, J. Liebert, & R. A. Saffer (Cambridge: CUP), 255
- Fusi Pecci, F., & Renzini, A. 1976, *A&A*, 46, 447
- Guarnieri, M. D., Ortolani, S., Montegriffo, P., Renzini, A., Barbuy, B., Bica, E., & Moneti, A. 1998, *A&A*, 331, 70
- Hartwick, F. D. A., Barlow, D. J., & Hesser, J. E. 1981, *AJ*, 86, 1044
- Iben, I., Jr. 1968, *Nature*, 220, 143
- Jacoby, G. H., Morse, J. A., Fullton, L. K., Kwitter, K. B., & Henry, R. B. C. 1997, *AJ*, 114, 261
- Kaisler, D., Harris, W. E., & MacLaughlin, D. E. 1997, *PASP*, 109, 920
- Kraft, R. P. 1994, *PASP*, 106, 553
- Kurucz, R. L. 1992, in *IAU Symp. 149, The Stellar Populations of Galaxies*, ed. B. Barbuy & A. Renzini (Dordrecht: Kluwer), 225
- Langer, G. E., & Hoffman, R. D. 1995, *PASP*, 107, 1177
- Layden, A. C. 1994, *AJ*, 108, 1016
- Layden, A. C. 1995, *AJ*, 110, 2312
- Mengel, J. G., & Gross, P. G. 1976, *Ap&SS*, 41, 407
- Ortolani, S., Bica, E., & Barbuy, B. 1994, *A&A*, 286, 444
- Piotto, G., et al. 1997, in *Advances in Stellar Evolution*, ed. R. T. Rood & A. Renzini (Cambridge: CUP), 84
- Reimers, D. 1975, *Mem. Soc. Roy. Sci. Liège*, 6th Series, 8, 369
- Renzini, A. 1977, in *Advanced Stages in Stellar Evolution*, ed. P. Bouvier & A. Maeder (Sauverny: Geneva Obs.), 149
- Rich, R. M., et al. 1997, *ApJ*, 484, L25

- Sandage, A. 1990, *ApJ*, 350, 631
- Sandage, A., & Wildey, R. 1967, *ApJ*, 150, 469
- Schramm, D. N. 1997, in *Critical Dialogues in Cosmology*, ed. N. Turok (Princeton: Princeton University Press), 81
- Shi, X. 1995, *ApJ*, 446, 637
- Silbermann, N. A., Smith, H. A., Bolte, M., & Hazen, M. L. 1994, *AJ*, 107, 1764
- Sosin, C., et al. 1997, in *Advances in Stellar Evolution*, ed. R. T. Rood & A. Renzini (Cambridge: CUP), 92
- Storm, J., Nordström, B., Carney, B. W., & Andersen, J. 1994, *A&A*, 291, 121
- Sweigart, A. V. 1997, *ApJ*, 474, L23
- Sweigart, A. V. 1998, in *The Third Conference on Faint Blue Stars*, ed. A. G. D. Philip, J. Liebert, & R. A. Saffer (Cambridge: CUP), 3
- Sweigart, A. V., & Catelan, M. 1998, in *ASP Conf. Ser. 135, A Half Century of Stellar Pulsation Interpretations: A Tribute to Arthur N. Cox*, ed. P. A. Bradley & J. A. Guzik (San Francisco: ASP), 39
- Sweigart, A. V., & Gross, P. G. 1976, *ApJS*, 32, 367
- van den Bergh, S. 1967, *AJ*, 72, 70

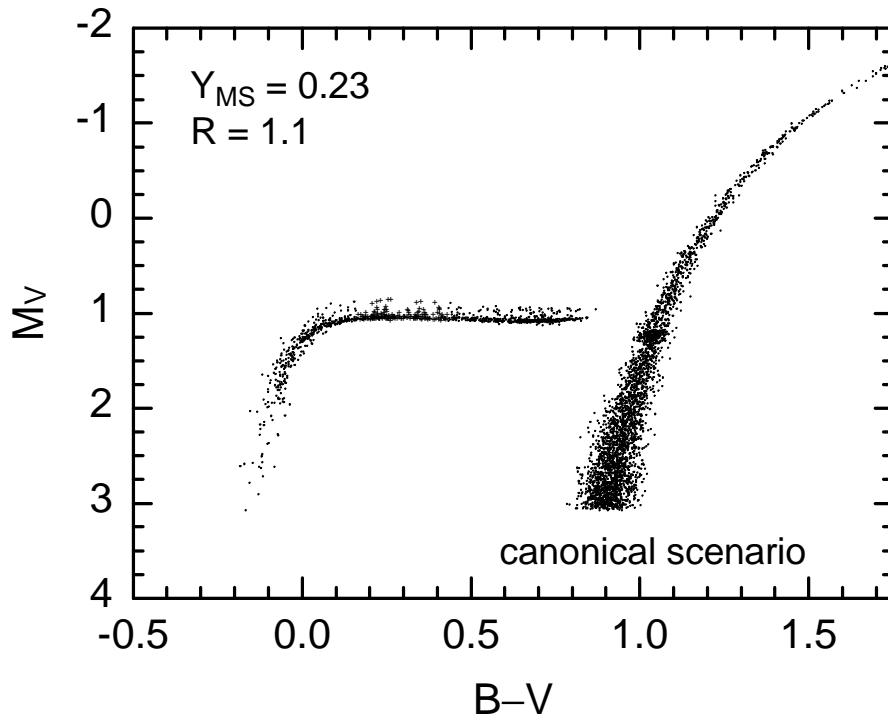


Fig. 1.— Canonical HB simulation for a helium abundance $Y_{\text{MS}} = 0.23$ and a heavy-element abundance $Z = 0.006$. Note that the HB is completely flat between $0.1 \lesssim B-V \lesssim 0.9$. The value of the ratio R between HB stars and RGB stars brighter than the mean RR Lyrae luminosity is indicated.

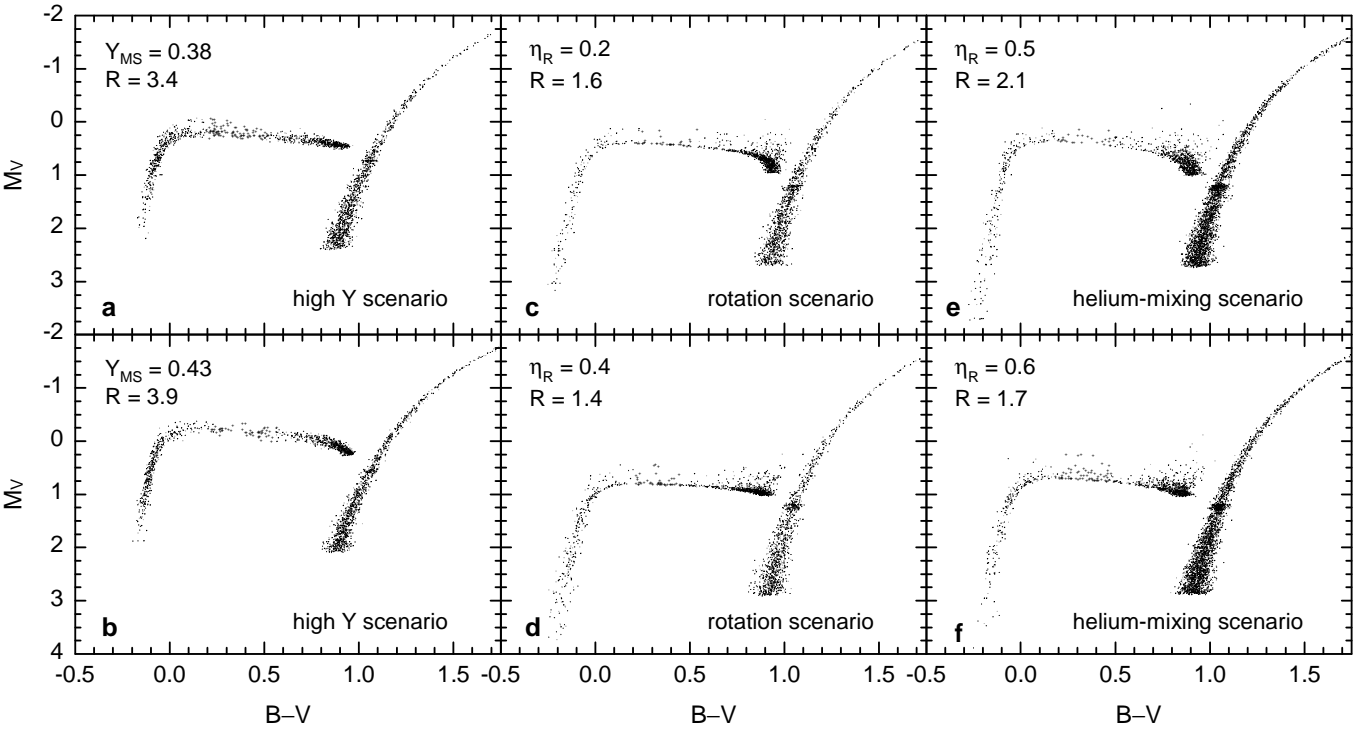


Fig. 2.— HB simulations for the high Y scenario with $Y_{\text{MS}} = 0.38$ (panel a) and $Y_{\text{MS}} = 0.43$ (panel b), the rotation scenario with the Reimers mass loss parameter $\eta_{\text{R}} = 0.2$ (panel c) and 0.4 (panel d), and the helium-mixing scenario with $\eta_{\text{R}} = 0.5$ (panel e) and 0.6 (panel f). The value of the R ratio is given in each panel. Note the upward slope of the HB with decreasing $B - V$.

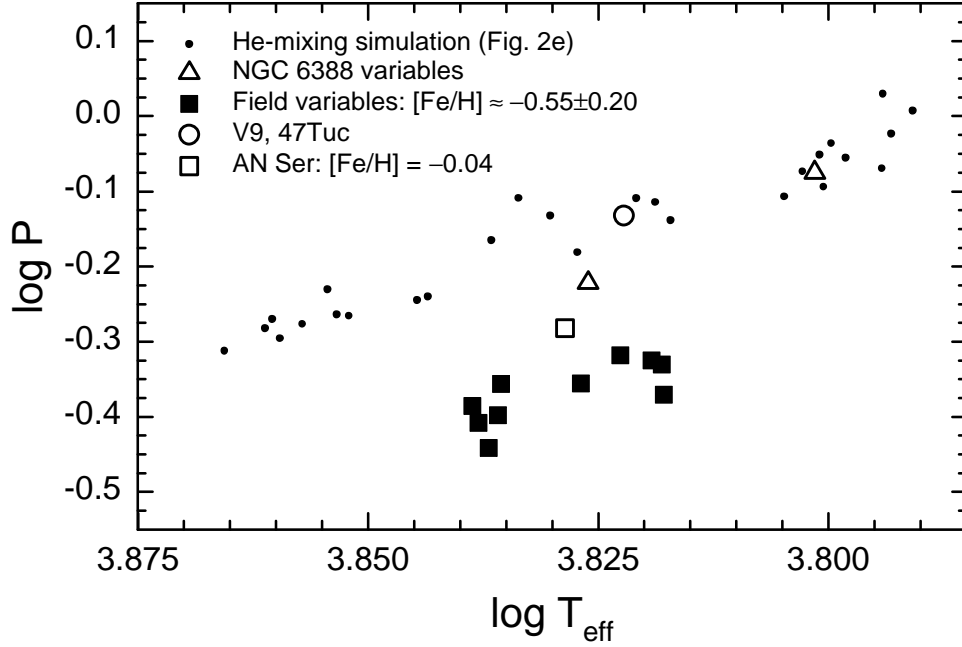


Fig. 3.— Period-temperature diagram for the RR Lyrae variables in NGC 6388 (\triangle) compared with field variables of similar metallicity (\blacksquare), V9 in 47 Tuc (\circ) and the very metal-rich, long-period field RR Lyrae variable AN Ser (\square). Model predictions for the simulation in Fig. 2e are shown as dots.